with a 25 percent oxygen loss at 690°C for $La_{1-x}Pb_xMnO_3$ and at 740°C for $Nd_{1-x}Pb_xMnO_3$ (*13*). These compounds are expected to be rather stable under the appreciably less reducing exhaust conditions in CAT I.

In earlier tests we obtained data on the efficacy of crushed single crystals of RE manganites in the oxidation of CO (*4*). Their activity was substantially improved by etching with dilute acids (tests 25 through 27 in Table 3). Conversions of 10 percent CO were reached at temperatures at least 50°C lower than those reported for unetched catalysts (*4, 14*). The activities of crushed single crystals of $La_{1-x}Pb_xMnO_3$ and $Nd_{1-x}Pb_xMnO_3$ ($x \simeq 0.3$) were not affected by the addition of 2 percent H_2O in tests in which mixtures of 16 percent CO and 8 percent O_2 in He were reacted at a space velocity of 8000 cm^3 of gas per hour per cubic centimeter of catalyst volume. We have also prepared very active catalysts by ceramic methods amenable to large-scale production (tests 28 through 33 in Table 3).

The conditions of our tests differ substantially from auto exhaust conditions in both concentration and space velocities. Our tests constitute only a preliminary evaluation of these catalysts for application in auto exhaust systems. The results of these and of a variety of other tests have led us to submit test samples of $La_{1-x}Pb_xMnO_3$ to several automotive companies. We suggest that the RE manganites should be evaluated as promising catalysts for the reduction of nitrogen oxides in auto exhaust, on the basis of (i) their low yield of NH_3, (ii) their good activity in the reduction of NO at relatively low temperatures, (iii) their stability under reducing as well as oxidizing conditions, and (iv) the fact that they have some measure of tolerance to lead (*4*). In fact, it seems feasible to develop these catalysts for use in the reducing as well as the oxidizing stages of catalytic exhaust converters.

R. J. H. VOORHOEVE
J. P. REMEIKA, D. W. JOHNSON, JR.
Bell Laboratories,
Murray Hill, New Jersey 07974

References and Notes

1. Clean Air Amendments of 1970, Public Law 91-604, section 6.
2. Committee on Motor Vehicle Emissions of the National Academy of Sciences, Semiannual Report to the Environmental Protection Agency (1 January 1972).
3. In the water gas shift reaction, H_2 is formed from H_2O and CO. See: J. H. Jones, J. T. Kummer, K. Otto, M. Shelef, E. E. Weaver, *Environ. Sci. Technol.* **5**, 790 (1971); R. L. Klimisch and G. J. Barnes, *ibid.* **6**, 543 (1972).
4. R. J. H. Voorhoeve, J. P. Remeika, P. E. Freeland, B. T. Mathias, *Science* **177**, 353 (1972). Further tests (made by R.J.H.V., J.P.R., and D.W.J) on the oxidation of CO at a space velocity of 60,000 cm^3 of gas per hour (at normal temperature and pressure) per cubic centimeter of catalyst, with 2 percent H_2O (by volume) in the gas feed, corroborated the conclusions of that earlier report. A 50 percent conversion of CO was reached at 300°C and a 95 percent conversion at 400°C.
5. D. B. Meadowcraft, *Nature* **226**, 847 (1970).
6. R. A. Baker and R. C. Doerr, *Ind. Eng. Chem. Process Des. Develop.* **4**, 188 (1965); M. Shelef and H. S. Gandhi, *Ind. Eng. Chem. Prod. Res. Develop.* **11**, 2 (1972).
7. R. L. Klimisch, paper presented at the 22nd Canadian Chemical Engineering Conference, Toronto, 17–20 September 1972.
8. This analysis was conducted by Ledoux and Co., Teaneck, N.J.
9. These honeycombs were corrugated structures (2.5 cm in diameter, 7.6 cm long) manufactured by the American Lava Corp.
10. The metal (99.999 percent pure) was obtained from United Mineral and Chemical Corp.
11. The results for Ru in Table 1 are similar to those obtained by Klimisch [see (*7*)] and by Shelef and Gandhi [M. Shelef and H. S. Gandhi, *Ind. Eng. Chem. Prod. Res. Develop.* **11**, 393 (1972), figure 2] for much more dilute mixtures of CO, NO, and H_2 at 230° to 375°C. If real exhaust is used, the results for Ru catalysts are generally much better; Ru is presently a favorite choice for CAT I, even its lifetime is reported to be limited [for example, see (*7*)]. We have no data that permit a comparison of Ru and the RE manganites under exhaust conditions.
12. Y. Henderson and H. W. Haggard, *Noxious Gases and the Principles of Respiration Influencing Their Action* (Reinhold, New York, 1943), pp. 99, 135, 149; M. Nicolet, in *Physics of the Upper Atmosphere*, J. A. Ratcliff, Ed. (Academic Press, New York, 1960), p. 27.
13. The extent to which these perovskite-like compounds can be reduced before they will decompose to form CoO, MnO, La_2O_3, and so on, is not known.
14. The possibility of etching these catalysts for the purpose of activating them is of interest also because such etching would remove lead deposits from a catalyst that had been used in an auto exhaust converter.
15. We thank L. E. Trimble for carrying out most of the tests reported here; P. K. Gallagher for discussions and for providing several precipitated oxides; M. Robbins for samples of $La_{0.5}Pb_{0.5}MnO_3$ with high surface area; Mrs. A. S. Cooper for x-ray analysis of several products; T. Y. Kometani for chemical analyses; F. Schrey for measuring the specific surface areas of the catalysts; and P. E. Freeland, D. J. Nitti, and J. J. Darold for assistance in the preparation and testing of catalysts. We also thank B. T. Matthias for supplying the initial impetus for this project and for his continuing interest and encouragement.

18 December 1972; revised 24 January 1973

Crystallographic Orientation of Clinoenstatite Produced by Deformation of Orthoenstatite

Abstract. *Uniaxial compression at 800°C and 5 kilobars confining pressure of a specimen cored from a single crystal of orthoenstatite [$(Mg,Fe)SiO_3$] produced fine lamellae 100 to 1000 angstroms thick of untwinned clinoenstatite. The two phases are joined along (100) planes and have* b *and* c *axes in common. The orientation of the clinoenstatite* a *axis contradicts several previously suggested transformation mechanisms and reduces the set of possible mechanisms by a factor of 2.*

The transformation of enstatite ($MgSiO_3$) from the orthorhombic to the monoclinic polymorph is dramatically promoted by shear stress on (100) planes parallel to the [001] direction (*1, 2*) but is only slightly promoted by hydrostatic pressure (*3*). A thermodynamic explanation of this effect has been given by Coe (*4*); it involves the assumption that the transition is macroscopically characterized by a reversible transformation strain of finite simple shear on (100) parallel to [001] through a well-defined angle. The actual displacement of atoms need not conform to simple shear in order to achieve the macroscopic deformation, but the movements of atoms must be coherent and long-range diffusion must be slow compared to the time required to accomplish the transformation. Metallurgists call such trans-

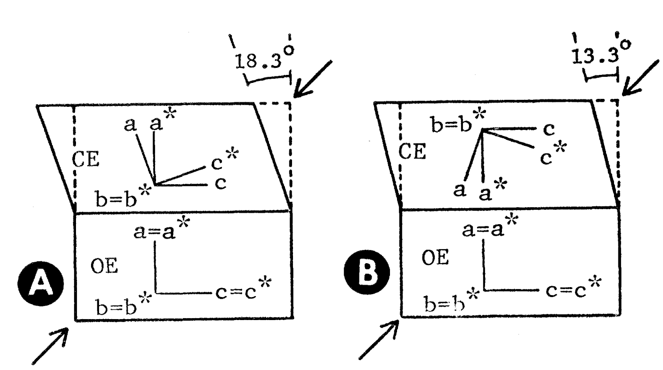

Fig. 1. Geometries for two mechanisms proposed for the transformation of part of a macroscopic piece of orthoenstatite (OE) to clinoenstatite (CE), showing the relation between the compression direction (arrows) and the direct (*a, b, c*) or reciprocal (*a**, *b**, *c**) crystallographic axes. (A) Mechanism of Brown *et al.* (*6*); (B) mechanism of Coe (*4*). The angles shown are the angles of macroscopic shear on (100) parallel to [001] (see text).

formations martensitic. The enstatite inversion is a special case in which the boundary between the two phases is the same as (or extremely close to) the shear plane (100) for the lattice correspondence and in which no additional lattice invariant shear is required (*5*).

Previous workers (*1, 2*) partially deduced the nature of the enstatite transition with the petrographic microscope. They found that the clinoenstatite (CE) formed during deformation experiments had *b* and *c* crystallographic axes in common with the parent orthoenstatite (OE) and had undergone plane shear on (100) parallel to [001]. They could not deduce the position of the *a* axis of the CE uniquely, however, because it was not known at that time whether the *Z* axis of the optical indicatrix lies within the acute or obtuse angle between the *a* and *c* crystallographic axes.

Several mechanisms have been proposed in which it is implicitly assumed that *Z* lies within the acute angle $a \wedge c$; these include a detailed description of atomic displacements by Brown *et al.* (*6*) involving a macroscopic shear of about 18.3° on (100) parallel to [001] (*1, 7*). Trommsdorff and Wenk (*8*), however, have suggested that *Z* more probably lies within the obtuse angle $c \wedge a$ in CE, as in other closely related monoclinic pyroxenes, in which case the above mechanisms all yield the wrong orientation of CE with respect to the compression direction and the corresponding sense of shear. Thus Coe (*4*) proposed a mechanism which yields the other orientation of CE (see Fig. 1). The mechanism is similar to that of Brown *et al.* but involves a smaller shear (about 13.3°) on (100) parallel to [001] and slightly greater atomic shuffles. In both mechanisms none of the Si-O bonds and half of the Mg-O bonds are broken.

We have used the electron microscope to determine the orientation of CE that was produced from OE during deformation. A cylindrical specimen 0.6 cm in diameter by 1.8 cm long was cored from a massive cleavage fragment of OE from Bamble, Norway, at about 45° to the *c* and *a* axes. Measurements of the angle $2V_\alpha$ on a universal stage with a petrographic microscope gave values around 86°, suggesting that about 14 mole percent of orthoferrosilite may be present in solid solution (*9*). If so, this specimen lies just outside the enstatite compositional range and should more correctly be called bronzite. The exact composition and thus the nomenclature appear to be unimportant for our purposes, however, because the isomorphous end member orthoferrosilite transforms under shear to clinoferrosilite in a manner quite analogous to enstatite (*10, 11*). Substitution of Ca^{2+} for Mg^{2+} and the appearance of other polymorphs at temperatures over 1000°C complicate the phase relations in these minerals, but these complications [which are summarized in a comprehensive review by Smith (*10*)] do not affect the present study.

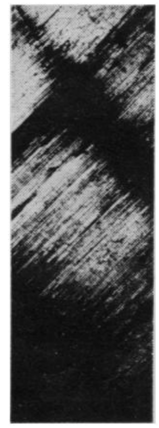

Fig. 2. Photomicrograph with crossed Nicol prisms of petrographic thin section parallel to (010) of enstatite specimen (0.6 cm in diameter by 1.8 cm long) after compression parallel to the length. The lineations at 45° to the length are traces of (100).

The specimen was shortened 3.7 percent at a strain rate of 10^{-4} sec^{-1} in a Griggs-type solid-medium deformation apparatus (*12*) with a confining pressure of 5 kbar and a temperature (near the center of the specimen) of 800°C. Optical examination after deformation of a petrographic thin section 30 μm thick cut parallel to (010) revealed a highly birefringent band of CE parallel to (100) with $Z \wedge c \cong 32°$ (*13*) and a kink band with the same properties which intersects it at about an 80° angle near one end of the core (see Fig. 2). In addition, large portions of the rest of the specimen show lesser degrees of transformation to CE.

For the study with a high-voltage (650 kv) transmission electron microscope, a suitably thin foil was prepared by ion-thinning (*14*) an area 2 to 3 mm in diameter from the nonkinked CE band of the petrographic thin section shown in Fig. 2. The method of preparation made it possible to identify the original orientation, so that the compression direction is known on the electron micrographs and diffraction patterns. The electron micrograph in Fig. 3B shows that what appeared optically in the petrographic thin section to be almost entirely CE is actually composed of submicroscopic lamellae, most of which range in thickness from 100 to 1000 Å. Such lamellae were also observed in two other less favorably oriented specimens deformed in preliminary experiments (*15*). They do not appear in naturally occurring, undeformed Bamble enstatite, although there are stacking faults parallel to (100) in some areas (see Fig. 3A).

The selected-area diffraction pattern in Fig. 3C shows a strong set of reflections which index as CE and a weaker set which index as OE (*16*). Correlation with bright- and dark-field electron micrographs establishes that the lamellae are alternately OE and untwinned CE in contact on (100) planes and with reciprocal axes a^* and b^* in common, in agreement with earlier petrographic and x-ray studies (*1, 2, 8*). Since $2|a^*|$ of OE equals $|a^*|$ of CE, the (200) reflections of OE coincide with the (100) reflections of CE (*16*). The orientation of the

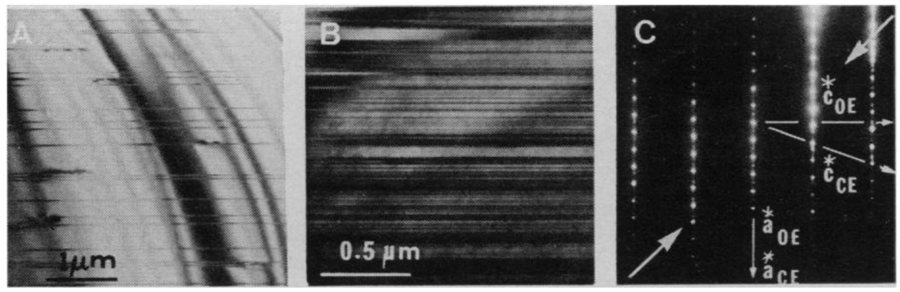

Fig. 3. High-voltage (650 kv) transmission electron microscope photographs of thin foils of Bamble enstatite with the *b* axis normal to page and the *c* axis east to west. (A) Bright-field micrograph of undeformed specimen showing OE with stacking faults parallel to (100). (B) Bright-field micrograph of a CE-rich portion of the deformed specimen of Fig. 2 (see text), showing alternating lamellae parallel to (100) of untwinned OE and CE. (C) Selected area diffraction pattern corresponding to B, showing the relation of the OE and CE reciprocal axes to each other and to the compression directions (heavy arrows). The origin of coordinate system is displaced from (000) to (12.00) of CE in order to show more clearly the OE reflections that differ from CE reflections.

c^* axis of CE with respect to the compression direction shown in Fig. 3C is that suggested by the optical measurements of Trommsdorff and Wenk (*8*) and favored in the mechanism of Coe (*4*) (compare Fig. 3C with Fig. 2). Comparison with our own optical measurements establishes that Z does lie in the obtuse angle between c and a.

In addition to the lamellae in the deformed specimens we see a variety of dislocations, most of which lie in the (100) planes of the boundaries of the lamellae. These probably reduce the strain energy due to atomic mismatch of the two phases, and may possibly assist in the transformation. Their Burgers vectors have not yet been determined. Dislocations are also required to accomplish the additional plastic strain which occurs during deformation because of the constraints imposed by the relatively rigid end pieces and because of the effects of friction at the surface of the specimen.

Further work is needed to clarify the nature of the dislocations and to better understand their role, if any, in the transformation mechanism. In addition, the angle of shear associated with the transition has not been determined. This would require the measurement of the angle through which some marker line $[u0w]$ (with $u \neq 0$) in the (010) plane is rotated by the transformation of OE to CE. Finally, we do not know yet whether the transformation of CE back to OE can proceed by a coherent mechanism which is the reverse of that for the transformation of OE to CE.

R. S. Coe

Earth Sciences Board, University of California, Santa Cruz 95060

W. F. Muller*

Department of Materials Science and Engineering, University of California, Berkeley 94720

References and Notes

1. F. J. Turner, H. Heard, D. T. Griggs, *Int. Geol. Congr. Rep. Sess. Norden 21st* (1960), part 18, p. 399.
2. C. B. Raleigh, *Science* **150**, 739 (1965); I. Borg and J. Handin, *Tectonophysics* **3**, 249 (1966); R. E. Riecker and T. P. Rooney, *Geol. Soc. Amer. Bull.* **78**, 1045 (1967); J. L. Munoz, *Carnegie Inst. Washington Yearb.* **66**, 369 (1968); C. B. Raleigh, S. H. Kirby, N. L. Carter, H. G. Avé Lallemant, *J. Geophys. Res.* **76**, 4011 (1971).
3. C. B. Sclar, L. C. Carrison, C. M. Schwartz, *Trans. Amer. Geophys. Union* **45**, 121 (1964); F. R. Boyd and J. L. England, *Carnegie Inst. Washington Yearb.* **64**, 117 (1965); J. Grover, *Trans. Amer. Geophys. Union* **53**, 539 (1972).
4. R. S. Coe, *Contrib. Mineral. Petrol.* **26**, 247 (1970).
5. C. M. Wayman, *Introduction to the Crystallography of Martensitic Transformations* (Macmillan, New York, 1964), p. 162. In these respects, the ortho- to clino-transition in enstatite is like the transition from hexagonal close-packed to face-centered cubic stacking in cobalt (see text).
6. W. L. Brown, N. Morimoto, J. V. Smith, *J. Geol.* **69**, 609 (1961).
7. J. Starkey, *Contrib. Mineral. Petrol.* **19**, 133 (1968).
8. V. Trommsdorff and H.-R. Wenk, *ibid.*, p. 158.
9. W. A. Deer, R. A. Howie, J. Zussman, *Rock Forming Minerals* (Longmans, London, 1963), vol. 2, p. 28.
10. J. V. Smith, *Mineral. Soc. Amer. Spec. Pap. No. 2* (1969), p. 3.
11. D. H. Lindsley and J. L. Munoz, *Carnegie Inst. Washington Yearb.* **67**, 86 (1969).
12. D. T. Griggs, *Geophys. J. Roy. Astron. Soc.* **14**, 19 (1967). Our apparatus is a later version, similar to but not exactly the same as that described in this article.
13. These are the optical properties that previous workers (*1*, *2*) have used to identify CE produced by shearing. In addition, we have checked the x-ray powder diffraction pattern for our CE. It is essentially the same as that listed in the powder diffraction file of the American Society for Testing Materials for "low" CE, and determined by D. A. Stephenson, C. B. Sclar, and J. V. Smith [*Mineral. Mag.* **35**, 838 (1966)].
14. R. Castaing, *Rev. Met. Paris* **52**, 669 (1955); J. D. Barber, *J. Mater. Sci.* **5**, 1 (1970); S. V. Radcliffe, A. H. Heuer, R. M. Fisher, J. M. Christie, D. T. Griggs, *Geochim. Cosmochim. Acta* **1** (Suppl. 1), 731 (1970); H. Bach, *J. Non-Cryst. Solids* **3**, 1 (1970). The electron microscopy was done with the Hitachi HV 650 instrument at the University of California, Berkeley, in the laboratory of G. Thomas.
15. These deformation experiments were kindly carried out by H.-R. Wenk at the University of California, Berkeley, at strain rates of 10^{-4} and 10^{-5} sec^{-1}. Because (100) was almost normal to the compression direction, the resolved shear stress on (100) was low and the transformation to CE less developed.
16. Reflections which are systematically extinct or very weak in an x-ray precession photograph are often present in the corresponding electron diffraction pattern because of the phenomenon of multiple reflection [K. W. Andrews, D. J. Dyson, S. R. Keown, *Interpretation of Electron Diffraction Patterns* (Plenum, New York, 1967)]. Thus, in Fig. 3C we see reflections corresponding to (100) planes of CE (bright spots, 9 Å spacing) and (100) planes of OE [weak spots where they do not coincide with (100) planes of CE, 18 Å spacing], whereas they are absent in x-rays precession photographs (*8*).

17. R.S.C. acknowledges support by NSF grant GA-25165 and an Alfred P. Sloan Foundation fellowship, and thanks H. M. Snyder for help with the deformation experiments. W.F.M. thanks the Deutsche Forschungsgemeinschaft for his research stipend, acknowledges support by the U.S. Atomic Energy Commission through the Lawrence Radiation Laboratory, Berkeley, and is greatly indebted to G. Thomas for hospitality and advice during his stay at Berkeley.

* Present address: Mineralogische Institut der Universität Frankfurt, Institut für Kristallographie, D-6 Frankfurt a.M., Germany.

25 October 1972; revised 18 January 1973

Teleconnections in the Equatorial Pacific Ocean

Abstract. *Geostrophic water transport by the equatorial countercurrent is compared with the observed sea level difference between two pairs of islands situated north and south of the current. The high correlation between the transport and the sea level difference makes it possible to construct a time series for the countercurrent transport over a 21-year period. The countercurrent carries warm water into the eastern tropical Pacific, and fluctuations in its strength give rise to temperature anomalies off Central America. Periods of exceptionally high transport by the countercurrent in the western Pacific coincide with the occurrence of El Niño several thousand kilometers downstream and demonstrate the existence of teleconnections between events in the Pacific Ocean.*

The transport of ocean water by a major ocean current such as the equatorial countercurrent can be monitored by such simple measurements as those of sea level on its northern and southern flanks. Fluctuations in the transport have a pronounced effect on temperatures off Central America. When transport is strong for a period of several months it contributes to the occurrence of El Niño off Peru (*1*). Such teleconnections have been found in the atmosphere by Bjerknes (*2*) but, I believe, have not before been established in the ocean.

The equatorial countercurrent flows eastward between about 4°N and 10°N across the entire Pacific Ocean, transporting warm water from west to east. The flow in the countercurrent is in approximate geostrophic balance (*3*) and occurs between a ridge near 4°N and a trough near 10°N in the sea surface topography (*4*). The average rate of transport decreases almost linearly from 40 megatons per second in the west to 10 megatons per second in the east (*5*), but individual values are highly variable. The associated difference in the height of sea level between the ridge and the trough varies between about 30 and 10 cm (*6*).

This geostrophic sea level difference can be measured by means of sea level gauges on islands situated in the topographic trough on the northern flank of the countercurrent and in the ridge on its southern flank. A strong relationship exists between the flow in the countercurrent and the sea level difference at stations near the equator and near 10°N (*7*). There are only two sea level stations near the equator, Christmas Island (2°N, 157°W) and Canton Island (3°S, 172°W). A good correlation ($r = 0.85$) exists between values of the monthly mean sea level at the two stations for a period of 12 years, when simultaneous records are available. The mean seasonal variation shown in Fig.